Electronic Supplementary Material (ESI) for RSC Advances.

Supplementary Information

Fabrication of 50-nm scale Pt nanostructures by block copolymer (BCP) and its characteristics of surface-enhanced Raman scattering (SERS)

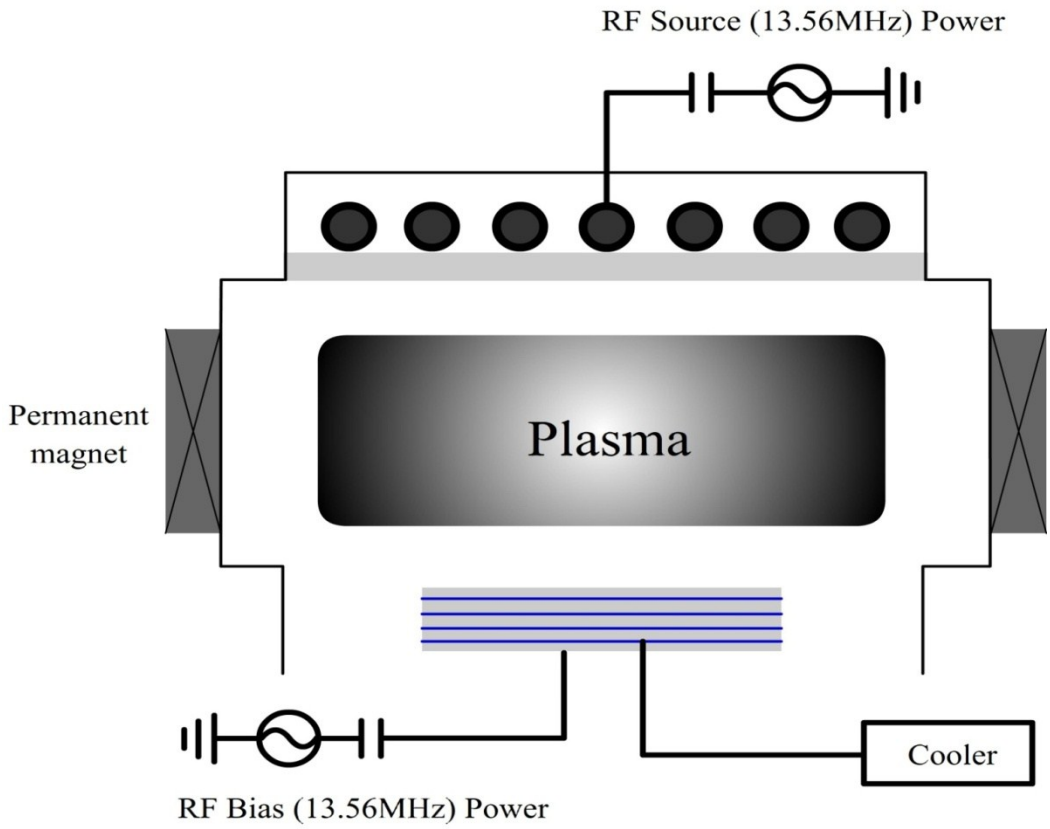

Figure S1. Schematic diagram of the ICP system used in the experiment

Figure S1 shows the schematic diagram of the magnetically-enhanced inductively-coupled plasma (ICP) system used in this study. This ICP source has eight permanent magnets arranged outside of the chamber wall to form a cusped magnetic field configuration. By using the ICP, we could obtain decreased electron loss to the chamber wall and increased plasma density. We connected the ICP source to 13.56 MHz rf power, and we also connected to a separate 13.56 MHz rf power. We maintained the substrate at room temperature. Using this ICP system for Pt nanostructure formation, we performed the sulfurization process, dry development process (PMMA removal for the BCP lithography), and selective etching of silicon and Pt.

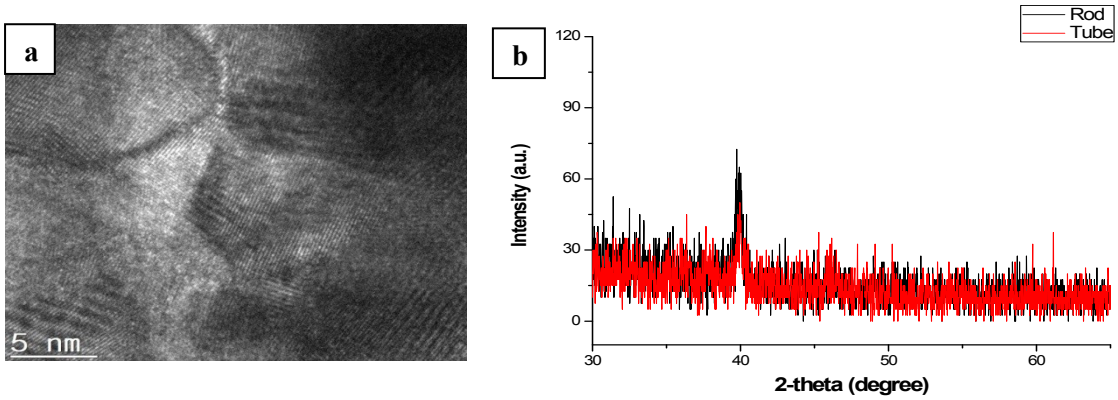

Figure S2. (a) High resolution TEM images of Pt materials deposited by ALD on flat surface and (b) XRD peak intensities of Pt nanorod and Pt nanotube deposited by ALD.

Figure S2 shows the high resolution TEM images of Pt deposited by ALD and (b) XRD peak intensities of Pt nanorod and Pt nanotube deposited by ALD. As shown in the figure, the Pt deposited by ALD was polycrystalline Pt with the preferred orientation of (111).

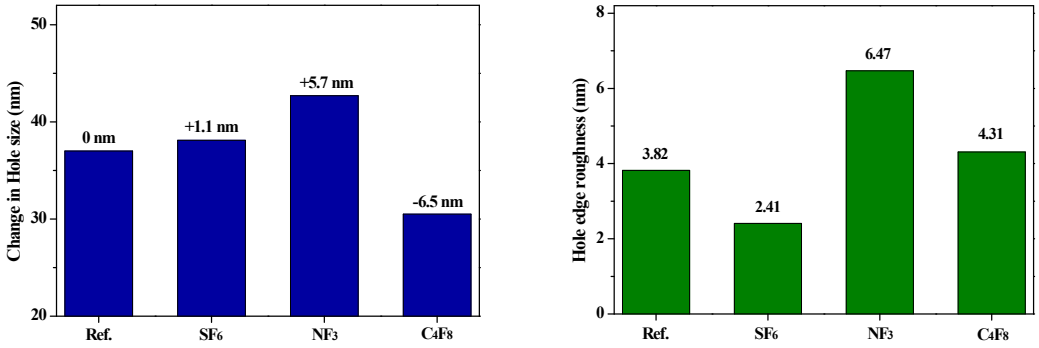

Figure S3. Changes in the PS hole size and hole edge roughness after various plasma surface treatments for the PS mask hardening

Figure S3 shows changes to the PS hole size and hole edge roughness measured after various plasma surface treatments for the PS mask hardening. We treated the PS hole pattern using sulfur and/or fluorine-containing plasmas without biasing the substrate (e.g., NF_3, C_4F_8, and SF_6) to harden the PS hole mask. We plasma-treated the PS hole pattern using these gases for 2 min under the following conditions: 13.56 MHz 50 W of ICP source power, 8 mTorr of operating pressure, and 76 sccm flow rate. Among these plasma treatments, the SF_6 plasma treatment exhibited the lowest change in hole size and the lowest hole edge roughness (even lower than that of the reference). For other plasma treatments using NF_3 or C_4F_8, both the PS hole size and the hole edge roughness increased. As a

method to check whether plasma-treated PS hole patterns hardened or not, we annealed the PS hole patterns treated with various plasmas at 190℃ for 15 min. The reference PS hole pattern and the PS hole pattern treated with NF_3 and C_4F_8 completely collapsed, while the PS hole pattern treated with SF_6 maintained the same PS hole shapes without changing the hole size (showing PS hardening) (not shown). To investigate whether the improvement related to fluorination or sulfurization of the PS, we also treated the PS hole pattern with an H_2S plasma under similar conditions, with the result showing similar improvement during the annealing (i.e., no change in the PS hole size after annealing, indicating a sulfurization effect). The hardening by the sulfurization appears to be related to the formation of SO_3H functional group in the PS, that is, sulfonation, as investigated by previous researches [1,2].

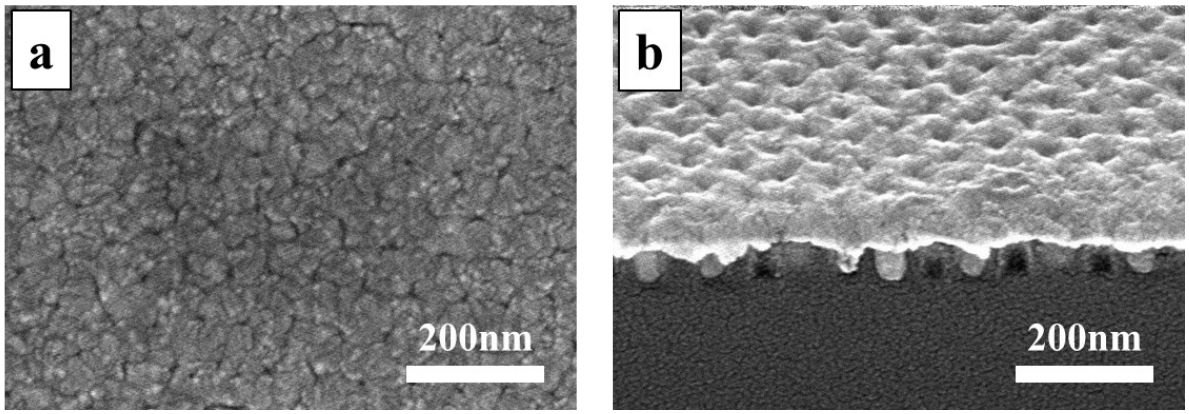

Figure S4. SEM micrographs after the deposition of 25-nm thick Pt in the 40-nm diameter silicon holes: (a) top view, and (b) tilted view of 50-nm deep silicon holes, after the deposition of 25-nm thick Pt by Pt ALD.

Figure S4 shows the SEM micrographs of silicon holes 40-nm in diameter and 50-nm deep, after the deposition of 25-nm thick Pt by Pt ALD. The deposition of 25-nm thick Pt completely filled all the 40-nm diameter silicon holes with Pt.

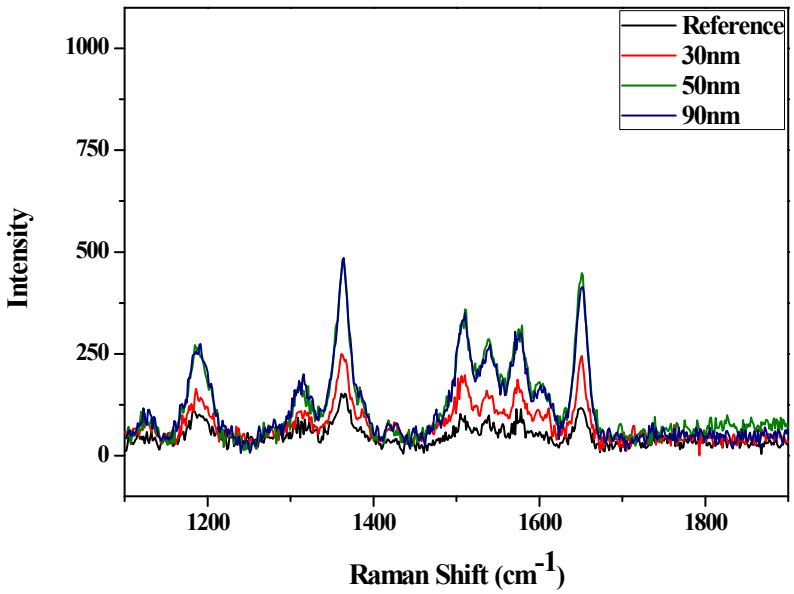

Figure S5. Raman intensities of rhodamine 6G with the concentration of 10^{-6} M on the silicon substrates with 12-nm diameter Pt nanohole arrays with different depths of 30, 50, and 90 nm. We also measured the Raman intensity on a flat Pt substrate, as the reference signal.

Using the silicon substrates with the Pt nanoholes with 12-nm diameter and 30~90 nm depth, we measured Raman intensities after coating with the rhodamine 6G solution with the concentration of 10^{-6} M. As a reference, we also measured the Raman intensity for a flat substrate deposited by Pt ALD. As shown, the Raman intensities with the Pt nanoholes were higher than that of the reference, possibly due to the electromagnetic enhancement at the nano-gap called a "hot spot" in the Pt nanoholes. The increase of Pt nanohole depth almost linearly increased the Raman intensity; however, in general, the SERS effect was not significant because the amplification ratio for the Pt nanoholes compared to the flat surface was only about 3~5 times.

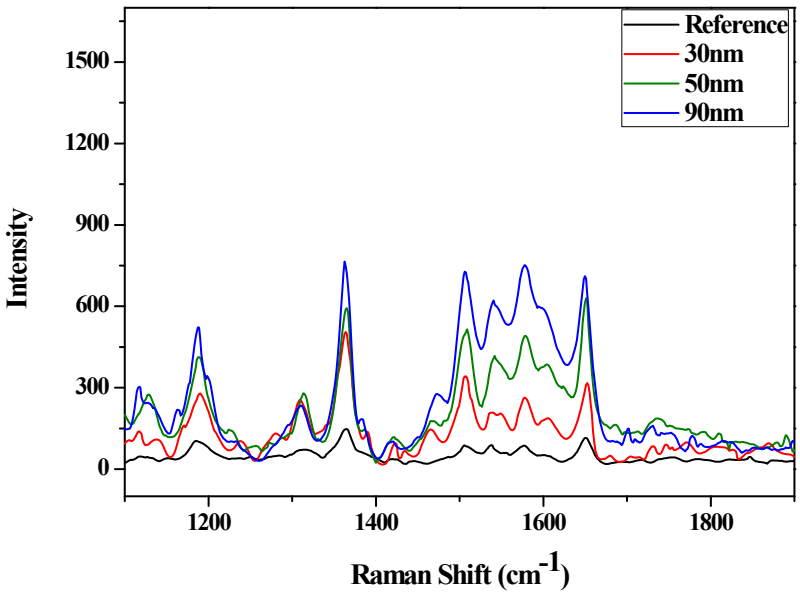

Figure S6. Raman intensities of rhodamine 6G with the concentration of 10^{-6} M on the silicon substrates with 40-nm diameter Pt nanorods with different depths of 30, 50, and 90 nm. We also measured the Raman intensity on a flat Pt substrate, as the reference signal.

Figure S5 shows Raman intensities measured using the silicon substrates with the 40-nm diameter and 30~90 nm height Pt nanorods with the rhodamine 6G solution having the concentration of 10^{-6} M. We also measured the Raman intensity of the reference for the flat substrate deposited by Pt ALD. As shown, the Raman intensities with the Pt nanorods were also higher than that of the reference, increasing almost linearly with the increased height of the Pt nanorods. The amplification ratios of the Pt nanorods for the same Pt height were higher than those with the Pt nanoholes, possibly due to more hot spots for the Pt nanorods.

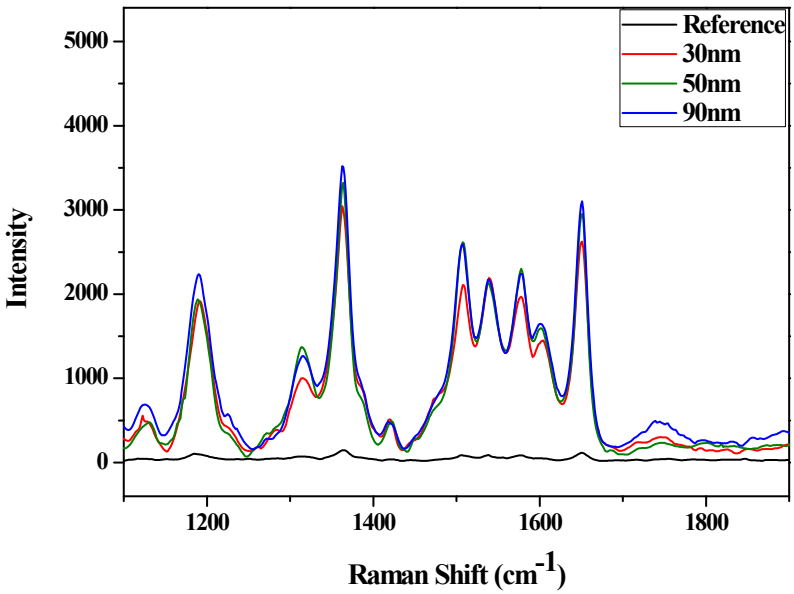

Figure S7. Raman intensities of rhodamine 6G with the concentration of 10^{-6} M on the silicon substrates with ~40 nm outside diameter and ~15 nm inside diameter Pt nanotubes with different depths of 30, 50, and 90 nm. We also measured the Raman intensity on a flat Pt substrate, as the reference signal.

We again measured Raman intensities of the rhodamine 6G using the silicon substrates with the Pt nanotubes having the different heights (30~90 nm). We observed more significant amplification of the Raman signal of about 3x 10^3 compared to that of the reference. The higher Pt nanotubes showed a higher amplification factor (similar to the cases of the Pt nanoholes and the Pt nanorods) even though the difference between the 30-nm high Pt nanotubes and the 90-nm Pt nanotubes was not significant, only showing 20% difference.

References

1 F. Kucera and J. Jancar, Polymer Engineering & Science, 2009, **49**, 1839-1845.

2 S. W. Choi, J. H. Shin, M. H. Jeon, J. H. Mun, S. O. Kim, G. Y. Yeom and K. N. Kim, Journal of nanoscience and nanotechnology, 2015, **15**, 8093-8098.